Real-Time Particle Size Analysis Using Focused Beam Reflectance Measurement as a Process Analytical Technology Tool for a Continuous Microencapsulation Process

Muhaimin Muhaimin (muhaimin_73@yahoo.de)
Universitas Jambi
Anis Yohana Chaerunisaa
Padjadjaran University
Roland Bodmeier
Freie Universität Berlin

Research Article

Keywords: Microparticles, FBRM, Particle size

Posted Date: May 20th, 2021

DOI: https://doi.org/10.21203/rs.3.rs-490815/v1

Abstract

The online real-time particle size analysis of the microencapsules manufacturing process using the continuous solvent evaporation method was performed using focused beam reflectance measurement (FBRM). In this paper, we use FBRM measurements to investigate the effects of polymer type and compare the size distributions to those obtained using other sizing methods such as optical microscope and laser diffraction. FBRM was also utilized to measure the length-weighted chord length distribution (CLD) and particle size distribution (PSD) online during particle solidification, which could not be done with laser diffraction or nested sieve analysis. The chord lengths and CLD data were taken at specific times using an online FBRM probe mounted below the microparticle. The timing of the FBRM determinations was coordinated with the selection of microparticle samples for particle size analysis by optical microscope and laser diffraction calculation as a reference. For all three produced batches tested, FBRM, laser diffraction, and sieve analysis yielded similar results. Hardening time for the transformation of emulsion droplets into solid microparticles occurred within the first 10.5, 19, 25, 30, and 55 minutes, according to FBRM results. The FBRM CLDs revealed that a larger particle size mean resulted in a longer CLD and a lower peak of particle number. The FBRM data revealed that the polymer type had a significant impact on microparticle CLD and the transformation process.

Introduction

Microencapsulation is a typical unit operation used in the production of solid dosage types including tablets, capsules, and sachets. Microparticle friability, microparticle flowability, tablet weight variance, tabletability, microparticle bulk density, tablet porosity, and tablet dissolution rate are all important parameters to consider.[1–5] The requirement to ensure the manufacture of a repeatable product necessitates the ability to produce microparticulate particle sizes and distributions within defined limits.[1–5]

When using solvent evaporation techniques to prepare microparticles, the speed of microparticles is a crucial factor that significantly affects drug release.[3] Slow hardening of droplets or emulsions causes drug compound diffusion, resulting in poor encapsulation content.[1,3,6–10] The hardening speed of microparticles in the solvent evaporation cycle is affected by the solubility of the polymer in organic solvents, which impact on microparticle properties such as particle size, volume of encapsulated drugs, matrix porosity, solvent residues, and initial drug release.[3] Polymers with various physical properties (such as solubility, molecular weight, reactivity, viscosity, biodegradability, permeability, and so on) have been applied to create microparticles.[11–15]

In the emulsification phase of a heterogeneous polymerisation device, particle size and particle size distribution are important.[14–17] The laser light scattering method has been used extensively to measure certain parameters. Optical miscroscopes were used in the traditional system. Dilution and sampling are used in these processes, which can result in changes in the droplet/particle size distribution due to break-up/coagulation or coalescence. Sampling techniques are often non-representative and can be used with

caution. The Focused Beam Reflectance Method (FBRM) technique allows for in-situ measurements to monitor particle/droplet size in real time during the microencapsulation process.[18] Lasentec invented the FBRM process, which can quantify particle size in the range of 0.1–1000 m. This instrument provides data from on-line and real-time measurements, allowing particle size data and suspension population patterns to be observed. It's been largely applied to monitor crystallization processes. This device can also visually track the transformation of emulsion droplets into stable microparticles, known as hardening time. Crystallization, flocculation, sludge conversion, polymorphic transformation, particle interference, microparticle solidification, and solubilization are some of the other processes that can be controlled using FBRM.

Microparticle particle size is measured using laser diffraction and sieve analysis during the solvent evaporation process. Sieve measurement equipment is cheap, and it is still commonly applied on the internet and for quality monitoring. While sieve analysis is the most common tool for microparticulate particle size analysis in the pharmaceutical industry, it is time consuming and difficult to conduct for oily or cohesive powders, microparticulate, or granules with particle sizes less than 25 micrometers. The process is not readily repeatable if the particles retained on some sieve are aggregates rather than single particles. The second biggest particle dimension, as determined by analytical sieving, is affected by particle structure. [18–25]

Laser diffraction methods produce results rapidly, but they presume that the subject particle is a sphere, which isn't always the case, particularly for aggregates and granules with irregular shapes. In comparison to an analytical sieve apparatus, laser diffraction instrumentation is still comparatively costly. Inline real-time particle size estimation and input control is an ideal method of microparticulate size analysis because it reduces human error, reduces analytical time and expense, reduces manufacturing cycle time, increases material throughput, and improves microparticulate size control. [23–25]

Since emulsifying the organic phase into an external aqueous phase, the solvent evaporation process causes particle size variations and compaction of the emulsion droplets. FBRM will monitor the mechanism and see which parameters can be tweaked to improve drug release or encapsulation performance. The calculation relies on the reflection of microparticles and is highly reliant on the particles' optical properties. [20–26]

Without the necessity for a pre-dilution side-stream, FBRM allows for in-line estimation of the particle size distribution of scattered particles within a moving fluid. It does not necessitate sampling, which could alter the particle size distribution due to dissolution or aggregation. The FBRM signal is highly dependent on the surface properties of the sample being measured, but it is a useful tool for monitoring the phase. [18,21,27–32]

Crystallization control, flocculation process design, slurry transfer, polymorphic transition tracking, particle disturbance control, microparticle solidification, and solubility measurements are only a few of the applications that have been identified using FBRM.[23,25,33–39] Despite the fact that several experiments

on FBRM have been published in the literature, no online monitoring of the development of microparticles using various polymers has ever been published using FBRM. In light of this, the aim of this study was to examine the ability of FBRM to be used for online monitoring of the shift in the microparticle CLD and detecting the transformation of emulsion droplets into solid microparticles during the solvent evaporation process, as well as to measure the particle size of microparticles with results that are as accurate as those measured by other methods. During the solvent evaporation process, the impact of polymer type on the solidification rate of polymeric microparticles/microparticle blends and particle size/ particle size distribution of emulsion droplets/hardened polymeric microparticles was also investigated. Hardening speed of microparticles, particle size and its distribution of emulsion droplets, and hard microparticles/microparticle blends produced by O / W using different polymers were the parameters examined.

Results And Discussion

Real-time particle size and particle size distribution analyses

For a quantitative study of microparticle particle size, FBRM was used. The findings of the FBRM measurement relative to those obtained using an optical microscope and laser diffraction revealed that there were no variations in particle size of microcapsules as compared to those obtained using an optical microscope or laser diffraction (Table 1).

Table 1
Effect of polymer type on particle size mean of microparticles

Polymer	Particle size mean (µm) (± SD)		
	FBRM	Optical microscope	Laser diffraction
Ethyl cellulose 4 cp	83.24 (± 5.28)	88.78 (± 7.64)	84.65 (± 6.11)
Eudragit RL 100	73.42 (± 6.44)	79.62 (± 9.17)	75.37 (± 5.75)
Eudragit RS 100	59.36 (± 5.21)	63.96 (± 8.92)	60.14 (± 6.44)
Polycaprolactone (Mw. 10000)	51.29 (± 4.09)	57.86 (± 8.12)	53.46 (± 5.32)
PLGA (RG503H)	64.08 (± 3.18)	68.15 (± 6.95)	65.75 (± 4.37)

Furthermore, FBRM can be applied to track the change in chord length distributions (CLD) at different levels of microparticle ripening in real time. It can track the shape of microparticles, particle size changes, hardening rate, particle properties, and chord length distribution.

In microparticulate systems, the solidification rate of polymeric microparticles is a significant parameter that influences particle size, encapsulation strength, and the initial burst.[12] Diffusion of the drug material out of the droplets and precipitation in the exterior phase will result from a very slow hardening of the emulsion droplets. The affinity between the solvent and the exterior phase, as well as the phase ratio, can influence the precipitation kinetics of the polymer solution droplets.

The solubility of the polymer in organic solvents influences the hardening speed of microparticles during the solvent evaporation process, which impacts on microparticle properties including particle size, amount of encapsulated drugs, matrix porosity, solvent residues, and initial drug release.[3] Microparticles have been created using a variety of polymers with various physical properties (such as solubility, molecular weight, reactivity, viscosity, biodegradability, permeability, and so on). Poly(-caprolactone), poly(lactic-co-glycolic acid), Eudragit RS 100, Eudragit RL 100, and ethyl cellulose microparticles are only a few of the materials accessible.[4–10]

Biocompatible and biodegradable polyesters include poly(-caprolactone) (PCL) and poly(lactic-co-glycolic acid) (PLGA).[4,5,9] Eudragit RS 100 and Eudragit RL 100 are methacrylic acid ester-free quaternary ammonium copolymers of ethyl acrylate and methyl methacrylate.[10] Eudragit RL 100 is more permeable than Eudragit RS 100 since it incorporates more co-trimethylammonioethyl methacrylate chloride. Ethyl cellulose is a non-biodegradable hydrophobic polymer.[11–15] The microparticle hardening rate of these polymers is unknown. As a result, it's important to understand how polymer properties affect the hardening time of polymeric microparticles.

As a function of time, the square weighted mean chord length of polymeric microparticles is plotted (Fig. 1a). All of the polymers formed small particles (less than 300 m).During solvent evaporation, various types of polymers applied in the formulation of polymeric microparticles result in a different square weighted mean (particle size). FBRM initially observed significant droplet sizes of all types of polymers when the organic polymer solution was emulsified. On both types of polymers, increasing the process time culminated in a decrease in particle size followed by a plateau size where the particle size remained unchanged. The particle size mean of microparticles when ethyl cellulose was utilized was greater than the others. The viscosity of the polymer solution has an effect on it. The high viscosity of Ethyl cellulose emulsion droplets reduced the organic phase's dispersibility in the aqueous media, resulting in larger particles. The viscosity data for polymer solutions can be found in.

The solubility of the polymer in the solvent affected the solidification rate of polymeric microparticles. The solubilities of polymers in dichloromethane were contrasted in this study (Table 2). In dichloromethane, ethyl cellulose (EC) had the lowest solubility, while polycaprolactone had the highest. As a result, polycaprolactone-based microparticles hardened at a slower rate than the others. Due to its poor solubility, ethyl cellulose has the highest hardening rate. In dichloromethane, Eudragit RL 100, Eudragit RS 100, and PLGA (RG503H) is more soluble than ethyl cellulose. [7,25,40–42] These properties cause microparticles to solidify at a slower rate than ethyl cellulose. The solidification of polymers with high solubilities took longer. They remained in the semi-solid state for longer, and it scattered more densely before fully solidifying, resulting in denser microparticles. In dichloromethane, Eudragit RL 100, Eudragit RS 100, and PLGA (RG503H) is more soluble than ethyl cellulose. These properties cause microparticles to solidify at a slower rate than ethyl cellulose. The solidification of polymers with high solubilities took longer.[3] They remained in the semi-solid state for longer, and it scattered more densely before fully solidifying, resulting in denser microparticles.[3,6]

Table 2
Effect of polymer type on solubility in dichloromethane, viscosity of polymeric solution and particle size mean of microparticles

Polymer	Solubility (g/ml) (± SD)	Viscosity (cSt) (± SD)	Hardening time (min)
Ethyl cellulose 4 cp	0.86 (± 0.03)	10.31 (± 1.14)	10.5
Eudragit RL 100	1.04 (± 0.04)	4.72 (± 0.83)	25
Eudragit RS 100	1.42 (± 0.02)	3.84 (± 0.39)	19
Polycaprolactone (Mw. 10000)	1.89 (± 0.05)	3.15 (± 0.45)	55
PLGA (RG503H)	1.25 (± 0.06)	4.36 (± 0.52)	30

For both polymers, the droplet shrinkage may be divided into two phases. Within 9 minutes (EC), 15 minutes (Eudragit RS 100), 20 minutes (Eudragit RL 100), and 25 minutes (PLGA), the original droplet size shrank dramatically (RG503H). This was accompanied by a period with no further pronounced shrinkage, known as a discontinued or sluggish shrinkage phase (Fig. 1a). It shows that in the first (rapid) step, the solvent was rapidly removed, and that in the second (slow) phase, the embryonic microparticle droplets were transformed into stable microparticles. Polycaprolactone caused the droplet size decrease to occur for another 55 minutes, meaning that the embryonic microparticle droplets solidified between 50 and 55 minutes (Fig. 1a). The start of the plateau process for all polymers was 10.5 minutes (ethyl cellulose 4 cp), 25 minutes (Eudragit RL 100), 19 minutes (Eudragit RS 100), 55 minutes (polycaprolactone), and 30 minutes (PLGA (RG503H) based on FBRM results (Fig. 1b and Table 2).

As EC microparticles are extracted quickly with solvent (Fig. 1), the polymer solidifies quickly on the droplet surface,[16,28] resulting in diffuse scattering to some extent. The improvement in the FBRM signal must be interpreted as opacification shifts and particle solidification.

As a time function, the chord count or particle counts of polymeric microparticles reveal a curve (Fig. 2). FBRM initially observed lower chord counts as the organic polymer solution was emulsified; but, as the process time was increased, the chord counts increased, indicating an increase in particle counts, followed by a plateau period where the chord counts were stable. During the solvent evaporation process, Eudragit RL 100, PLGA (RG503H), Eudragit RS 100, and polycaprolactone showed identical chord counts profiles. The particle counts of ethyl cellulose microparticles is smaller than those of the other microparticles, owing to the processing of microparticles of the biggest size.
Eudragit RL 100, Eudragit RS 100, and PLGA (RG503H) had smaller particle sizes than ethyl cellulose, resulting in higher particle counts. The particle size of polycaprolactone was the lowest, but the particle count was not the largest. This is due to Polycaprolactone's particle properties, which create slightly transparent microparticles as opposed to other polymers (Fig. 5.d1). When a laser beam strikes a transparent microparticle, multiple reflections occur inside the microparticle, illuminating the whole

sphere. As a more opaque microparticle is struck by a laser pulse, the light is dispersed to the detector, resulting in a higher scattering value.[27,28,32,43] The backscattered signal is very strong due to the invisible microparticles' absorbance, resulting in a high degree of chord length (particle size) and low chord counts (particle counts).[44–46] This is in conjunction with Greaves et al., as well as Sparks and Dobbs, who concluded that only opaque and highly reflective droplets or microparticles (with microstructure on the surface) provide repeatable and consistent effects.[32,44,45]

The formation of microparticles-based polymer materials was clearly supported by real-time particle size analysis and particle size distribution experiments of all polymeric microparticles with in situ polymerization. Surprisingly, these findings suggest that, based on the polymer structures, all of the polymer products used various microparticle forming mechanisms.

At the same concentration, the chord length distributions (particle size distribution) of various polymers determined by FBRM is different (Fig. 3). Since the number of microparticles was reduced, larger microparticles resulted in longer chord lengths and a lower peak particle number. In this case, increasing the viscosity of the polymer solution resulted in a larger square weighted mean chord length (particle size) and a wider chord length distribution. Polycaprolactone solution (organic phase) had a lower viscosity than other polymers, resulting in smaller microparticles. In comparison to other polymeric microparticles, this polymer provided narrower square weighted mean chord lengths and narrow chord length distributions.

Figure 4. Comparison of the square weighted chord length distribution for various polymer obtained by the FBRM method (O/W) [at 4 hours stirring time]

Scanning electron microscopy (SEM) studies

Figure 5 shows a SEM photomicrograph of microparticles produced by the O/W process with the polymers ethyl cellulose (EC), Eudragit RL 100, Eudragit RS 100, polycaprolactone, and PLGA (RG503H) (Fig. 5. a2-e2 and a3-e3). Microparticles of ethyl cellulose (EC), polycaprolactone, and PLGA (RG503H) were spherical with smooth surfaces without aggregation, while those of Eudragit RL 100 and Eudragit RS 100 were spherical, oval, and needle shaped (mixture) with smooth surfaces without aggregation, according to the surface of microparticles without drug prepared by the O/W process. There were no pores on any of the microparticle surfaces (Fig. 5.a3-e3).

Because of the influence of the form and physical properties of the polymer, as well as its solubility in dichloromethane as a solvent, all microparticles possess varying levels of opacity (Fig. 5.a1-e1). Polymers with a high dichloromethane solubility took longer to solidify and remained in a semisolid state for longer. Before fully solidifying, the scattered process became more condensed. When the polymer matrix was shrunk for a longer period of time, the polymer matrix becomes thick, and the droplet gradually shrank into stable microparticles, leaving transparent droplets. Polymeric microparticles had a diameter ranging from 51 to 83 micrometers (FBRM) (Table 1). The mean particle size of microparticles made with a high viscosity polymer solution was greater than those made with a low viscosity solution.

This is due to faster solidification on the surface of embryonic microparticle droplets, resulting in accelerated microparticle droplet shrinkage. Based on the data, the square weighted mean chord lengths (particle size mean) determined by FBRM were better estimated than those calculated by microscopic observation, as shown by the data's lower standard deviation (Table 1).

Particle size analysis.

In the FBRM results, independent particle size analyses of microparticles and prepared polymeric microparticles are given (Fig. 1). The results showed that the final particle size measured did not vary as compared to the data collected by optical microscope and laser diffraction measurement (Table 1). It can be concluded that particle size measurement using the centered beam reflectance measurement (FBRM) method yields the same results as the method that has been evolved and proven with further advantages in terms of providing particle size data and population patterns of particles in suspension in real time and on-line. The FBRM technique allows for the measurement of parameter processes during particle forming without destroying the morphology or counts of the process's formed particles.

Conclusion

For all three processed batches analyzed, FBRM, laser diffraction, and sieve analysis revealed identical particle sizes. The FBRM approach has the advantage of being able to do in-situ particle size analysis in real time without sampling or dilution. During the solvent evaporation process, the FBRM was successfully used as an efficient and convenient process analyzer for either quantitative particle size estimation or qualitative online monitoring of the change in the microparticle chord length distribution (particle size distribution) of polymeric microparticles. The FBRM detects the transition of emulsion droplets into solid microparticles and agglomeration by detecting a shift in signal that is caused by particle surface characteristics and optical properties. Polymer type has a significant impact on microparticle size distribution, transformation, and agglomeration.

Experimental Section

Materials

All materials were of at least reagent grade and used as received: Ethocel (Standard 4 Premium, Colorcon Ltd, Kent, UK)); ethyl acrylate methyl methacrylate copolymer (Eudragit RS 100 and Eudragit RL 100, Evonik Röhm GmbH, Darmstadt, Germany), Poly(D,L-lactide-co-glycolide) (Resomer RG503H, Boehringer-Ingelheim Pharma GmbH & Co. KG, Ingelheim, Germany), Poly(ε-caprolactone) (PCL; Mn approx. 10000) (Sigma-Aldrich Chemie GmbH, Steinheim, Germany); polyvinyl alcohol (PVA, Mowiol 40–88, Kuraray Europe GmbH, Frankfurt, Germany); and dichloromethane (Carl Roth GmbH & Co. KG, Karlsruhe, Germany).

Viscosity measurement

7.5% w/v solution of Ethocel 4 cP, Eudragit RS 100, Eudragit RL 100, PLGA (Resomer RG503H) and poly(ε-caprolactone) in dichloromethane were analyzed using an Ostwald viscometer type 50111/Ia, instrument constant: K = 0.05152 mm^2/s^2 (Schott-Geräte GmbH, Hofheim, Germany) at 25 ^oC (n = 3). The viscosity were calculated as follows:

$v = K.t$

v : kinematic viscosity (mm^2/s or cSt)

K : instrument constant (mm^2/s^2)

t : flow time (s)

Microparticles preparation

The solvent evaporation method based on the formation of O/W emulsion was used to prepare microparticles. In the O/W-dispersion method, a solution of the polymer in dichloromethane (7.5% w/v) was dispersed into an external aqueous phase (800 ml 0.25% PVA solution). The emulsion was stirred for 4 h at 500 rpm with a propeller stirrer (Heidolph Elektro *GmbH* & Co. KG, Kelheim, Germany). After 4 h, the microparticles were separated from the external aqueous phase by wet sieving followed by washing with 200 ml deionized water, desiccator-drying for 24 h and storage in a desiccator.

On-line particle size analysis

FBRM probe (Lasentec FBRM D600T, Mettler Toledo AutoChem, Inc., Redmond, WA, USA) was immersed and positioned in the emulsification vessel (O/W emulsions). It was placed between the propeller stirrer and inner side of the mulsion vessel (2t, Fig. 6). This spot can provide good flow of turbulence, hence allowing a representative sample of the particle system to be measured. The measurement range of the FBRM D600T probe is 0.25 - 4000 µm. A propeller stirrer (Heidolph Elektro *GmbH* & Co. KG, Kelheim, Germany) was set at stirring speed of 500 rpm for 4 hours. The measurements were performed in triplicate every 10 seconds, during a period of 4 hours. The Lasentec FBRM D600T use a beam of laser light which rotated with constant speed of $2ms^{-1}$as source. The of laser energy is reflected back into the probe by backscatter from particles next to the sapphire window as an orifice. Fig. 6 shows the operating principle of the Lasentec FBRM probe.[19,23,46]

A detailed operating mechanism of the Lasentec FBRM technique is described by Kougoulos et al.[23] The measured particle size when a laser beam crosses the particle randomly for spherical, irregular and odd-shaped particles, shape and orientation will influence the measured particle size is described by Silva et al.[46] The operating mechanism of the Lasentec FBRM technique[23] and the measuring particle size when a laser beam crosses the particle randomly[46] is acknowledg

Figure 6. Schematic drawing of probe positioning relative to the impeller (1. Propeller stirrer; 2. Lasentec FBRM probe; 3. Processing unit; 4. PC monitoring the particle size distribution on-line) (a), and Examples

of the measured chord length (line) when a laser beam crosses (1) a spherical particle, (2 and 3) an oval particle in different positions and (4, 5, 6 and 7) an irregular particle in different positions – illustration of the effect of particle orientation on the obtained chord length (b).

Comparison of Average Particle Size by Various Techniques

Particle size distributions can be weighted and averaged in a variety of ways. Table 1 plots various length-weighted median FBRM, average sizes with values from laser diffraction and a range of sieved or cyclosized fractions. Calculated geometric average values from FBRM, laser diffraction and sieving are also included for comparison. Laser diffraction is alternative technique that covered the entire size range, but this is not meant to imply that the technique provides a more accurate particle size. A comparison of the median square-weighted chord lengths across all the sieved fractions also shows that the FBRM results were essentially unaffected by particle material. This is certainly not expected to be applicable to all materials, but is more a consequence of the relatively low aspect ratio of the polymer materials studied.

Characterization Techniques

Optical microscopy

Microparticles were spread on microscope slides and observed with an optical light microscope (Axiotrop 50, Carl Zeiss AG, Jena, Germany) equipped with an image analysis system (INTEQ Informationstechnik GmbH, Berlin, Germany) consisting of a digital camera (type MC1) and the EasyMeasure software (version 1.4.1).

Scanning electron microscopic studies

The external morphology of microparticles was analysed by scanning electron microscopy (SEM). For surface imaging, the microparticles were fixed on a sample holder with double-sided tape. All samples were coated under an argon atmosphere with fine gold to a thickness of 8 nm (SCD 040, Bal-Tec GmbH, Witten, Germany) in a high-vacuum evaporator. Samples were then observed with a scanning electron microscope (S-4000, Hitachi High-Technologies Europe GmbH, Krefeld, Germany).

Declarations

Acknowledgment

The financial support of Directorate General of Higher Education, Ministry of Research, Technology and Higher Education of the Republic of Indonesia for this research is acknowledged.

Author Contributions

M. M. Conceptualization, Investigation, Methodology, Visualization, Writing - original draft. A. Y. C. Writing - review & editing. R. B. Conceptualization, Methodology, Resources, Supervision.

References

1. Alhnan, M. A. & Basit, A. W. Engineering polymer blend microparticles: An investigation into the influence of polymer blend distribution and interaction. *Eur. J. Pharm. Sci.* **42**, 30–36 (2011).
2. Saralidze, K., Koole, L. H. & Knetsch M.L.W. Polymeric microspheres for medical applications. *Materials.* **3**, 3537–3564 (2010).
3. Spörl, J. M. *et al.* Ionic liquid approach toward manufacture and full recycling of all-cellulose composites. *Macromol. Mater. Eng.* **303**, 1–8 (2018).
4. Chen, D. R., Bei, J. Z. & Wang, S. G. Polycaprolactone microparticles and their biodegradation. *Polym. Degrad. Stabil.* **67**, 455–459 (2000).
5. Gibaud, S., Awwadi, N. J. A., Ducki, C. & Astier, A. Poly(ε-caprolactone) and Eudragit® microparticles containing fludrocortisone acetate. *Int. J. Pharm.* **269**, 491–508 (2004).
6. Li, H., Ma, Y., Li, Z., Cui, Y. & Wang, H. Synthesis of novel multilayer composite microcapsules and their application in self-lubricating polymer composites. *Compos. Sci. Technol.* **164**, 120–128 (2018).
7. Li, W. I., Anderson, K. W., Mehta, R. C. & DeLuca, P. P. Prediction of solvent removal profile and effect on properties for peptide-loaded PLGA microspheres prepared by solvent extraction/evaporation method. *J. Control. Rel.* **37**, 199–214 (1995).
8. Murtaza, G. Ethylcellulose microparticles: A review. *Drug Res.* **69**, 11–22 (2012).
9. Ray, A. M. L. *et al.* Vancomycin encapsulation in biodegradable poly(ε-caprolactone) microparticles for bone implantation. Influence of the formulation process on size, drug loading, in vitro release and cytocompatibility. *Biomaterials.* **24**, 443–449 (2003).
10. Trapani, A. *et al.* RS 100 microparticles containing 2-hydroxypropyl-β-cyclodextrin and glutathione: Physicochemical characterization, drug release and transport studies. *Eur. J. Pharm. Sci.* **30**, 64–74 (2007).
11. Duarte, A. R. C., Gordillo, M. D., Cardoso, M. M., Simplicio, A. L. & Duarte, C. M. M. Preparation of ethyl cellulose/methyl cellulose blends by supercritical antisolvent precipitation. *Int. J. Pharm.* **311**, 50–54 (2006).
12. Muhaimin, M. & Bodmeier, R. Data on the application of the focused beam reflectance measurement (FBRM): A process parameters dataset for the ethyl cellulose (EC) microparticles preparation by the solvent evaporation method. *Data in Brief.* **30**, 1–14 https://doi.org/10.1016/j.dib.2020.105574 (2020).
13. Pearnchob, N. & Bodmeier, R. Dry polymer powder coating and comparison with conventional liquid-based coatings for Eudragit® RS, ethylcellulose and shellac. *Eur. J. Pharm. Biopharm.* **56**, 363–369 (2003).
14. Muhaimin, M., Yusnaidar, Y., Syahri, W., Latief, M. & Chaerunisaa, A. Y. Microencapsulation of *Macaranga gigantea* leaf extracts: Production and Characterization.*Pharmacognosy Journal*. 12(4), (2020).

15. Saravanan, M. & Anupama, B. Development and evaluation of ethylcellulose floating microspheres loaded with ranitidine hydrochloride by novel solvent evaporation-matrix erosion method. *Carbohyd. Polym.* **85**, 592–598 (2011).
16. Freitas, S., Merkle, H. P. & Gander, B. Microencapsulation by solvent extraction/evaporation: reviewing the state of the art of microsphere preparation process technology. *J. Control. Rel.* **102**, 313–332 (2005).
17. O'Donell, P. B. & McGinity, J. W. Preparation of microspheres by the solvent evaporation technique. *Adv. Drug Delivery Rev.* **28**, 25–42 (1999).
18. Boxall, J. A., Koh, C. A., Sloan, E. D., Sum, A. K. & Wu, D. T. Measurement and calibration of droplet size distributions in water-in-oil emulsions by particle video microscope and a focused beam reflectance method. *Ind. Eng. Chem. Res.* **49**, 1412–1418 (2010).
19. Dowding, P. J., Goodwin, J. W. & Vincent, B. Factors governing emulsion droplet and solid particle size measurements performed using the focused beam reflectance technique. *Colloids Surf. A: Physicochem. Eng. Asp.* **192**, 5–13 (2001).
20. Heath, A. R., Fawell, P. D., Bahri, P. A. & Swift, J. D. Estimating average particle size by focused beam reflectance measurement (FBRM). *Part. Part. Syst. Char.* **19**, 84–95 (2002).
21. Kail, N., Marquardt, W. & Briesen, H. Estimation of particle size distributions from focused beam reflectance measurements based on an optical model. *Chem. Eng. Sci.* **64**, 984–1000 (2009).
22. Kirwan, L. J. Investigating bauxite residue flocculation by hydroxamate and polyacrylate flocculants utilising the focussed beam reflectance measurement probe. *Int. J. Miner. Process.* **90**, 74–80 (2009).
23. Kougoulos, E., Jones, A. G. & Kaczmar, M. W. Modelling particle disruption of an organic fine chemical compound using Lasentec focussed beam reflectance monitoring (FBRM) in agitated suspensions. *Powder Technol.* **155**, 153–158 (2005).
24. Leba, H., Cameirao, A., Herri, J. M., Darbouret, M. & Peytavy, J. L. Chord length distributions measurements during crystallization and agglomeration of gas hydrate in a water-in-oil emulsion: Simulation and experimentation. *Chem. Eng. Sci.* **65**, 1185–1200 (2010).
25. Muhaimin, M. & Bodmeier, R. Effect of solvent type on preparation of ethyl cellulose microparticles by solvent evaporation method with double emulsion system using focused beam reflectance measurement. *Polymer Int.* **66**, 1448–1455 (2017).
26. Wynn, E. J. W. Relationship between particle-size and chord-length distributions in focused beam reflectance measurement: stability of direct inversion and weighting. *Powder Technol.* **133**, 125–133 (2003).
27. Vay, K., Frieß, W. & Scheler, S. Understanding reflection behavior as a key for interpreting complex signals in FBRM monitoring of microparticle preparation processes. *Int. J. Pharm.* **437**, 1–10 (2012).
28. Yu, W. & Erickson, K. Chord length characterization using focused beam reflectance measurement probe - methodologies and pitfalls. *Powder Technol.* **185**, 24–30 (2008).
29. Zidan, A. S., Rahman, Z. & Khan, M. A. Online monitoring of PLGA microparticles formation using Lasentec focused beam reflectance (FBRM) and particle video microscope (PVM). *AAPS J.* **12**, 254–

262 (2010).

30. Kempkes, M., Eggers, J. & Mazzotti, M. Measurement of particle size and shape by FBRM and in situ microscopy. *Chem. Eng. Sci.* **63**, 4656–4675 (2008).
31. Simmons, M. J. H., Langston, P. A. & Burbidge, A. S. Particle and droplet size analysis from chord distributions. *Powder Technol.* **102**, 75–83 (1999).
32. Greaves, D. *et al.* Measuring the particle size of a known distribution using the focused beam reflectance measurement technique. *Chem. Eng. Sci.* **63**, 5410–5419 (2008).
33. Abbas, A., Nobbs, D. & Romagnoli, J. A. Investigation of on-line optical particle characterization in reaction and cooling crystallization systems, Current state of the art. *Measurement Sci. Technol.* **13**, 349–356 (2002).
34. Barrett, P. & Glennon, B. Characterizing the metastable zone width and solubility curve using Lasentec FBRM and PVM. *Trans IChemE.* **80**, 799–805 (2002).
35. Yu, Z. Q., Tan, R. B. H. & Chow, P. S. Effects of operating conditions on agglomeration and habit of paracetamol crystals in anti-solvent crystallization. *J. Cryst. Growth.* **279**, 477–488 (2005).
36. Sankaranarayanan, S., Likozar, B. & Navia, R. Real-time particle size analysis using the focused beam reflectance measurement probe for in situ fabrication of polyacrylamide–filler composite materials. *Sci. Rep.* **9**, 1–12 (2019).
37. Daymo, E. A., Hylton, T. D. & May, T. H. Acceptance testing of the Lasentec Focused Beam Reflectance Measurement (FBRM) monitor for slurry transfer applications at Hanford and Oak Ridge. Part of the SPIE Conference on Nuclear Waste Instrumentation and Engineering, Boston, Massachusetts. 3536, 82–92(1998).
38. O'Sullivan, B., Barrett, P., Hsiao, G., Carr, A. & Glennon, B. In Situ Monitoring of Polymorphic Transitions. *Organic Process Res. Develop.* **7**, 977–982 (2003).
39. Kim, Y. S., Rio, J. R. M. D. & Rousseau, R. W. Solubility and prediction of the heat of solution of sodium naproxen in aqueous solutions. *J. Pharm. Sci.* **94**, 1941–1948 (2005).
40. Turner, D. J., Miller, K. T. & Sloan, E. D. Direct conversion of water droplets to methane hydrate in crude oil. *Chem. Eng. Sci.* **64**, 5066–5072 (2009).
41. Kumar, V., Taylor, M. K., Mehrotra, A. & Stagner, W. C. Real-time particle size analysis using focused beam reflectance measurement as a process analytical technology tool for a continuous granulation-drying-milling process. *AAPS Pharm. Sci. Tech.* **14**, 523–530 (2013).
42. Yeo, Y. & Park, K. Control of encapsulation efficiency and initial burst in polymeric microparticle systems. *Arch. Pharmacal Res.* **27**, 1–12 (2004).
43. Wu, H., White, M. & Khan, M. A. Quality-by-Design (QbD): An integrated process analytical technology (PAT) approach for a dynamic pharmaceutical co-precipitation process characterization and process design space development. *Int. J. Pharm.* **405**, 63–78 (2011).
44. Sparks, R. G. & Dobbs, C. L. The use of laser backscatter instrumentation for the online measurement of the particle-size distribution of emulsions. *Part. Part. Syst. Char.* **10**, 279–289 (1993).

45. Scheler, S. Ray tracing as a supportive tool for interpretation of FBRM signals from spherical particles. *Chem. Eng. Sci.* **101**, 503–514 (2013).
46. Silva, A. F. T. *et al.* Particle sizing measurements in pharmaceutical applications: Comparison of in-process methods versus off-line methods.*Eur J Pharm Biopharm*(2013).

Figures

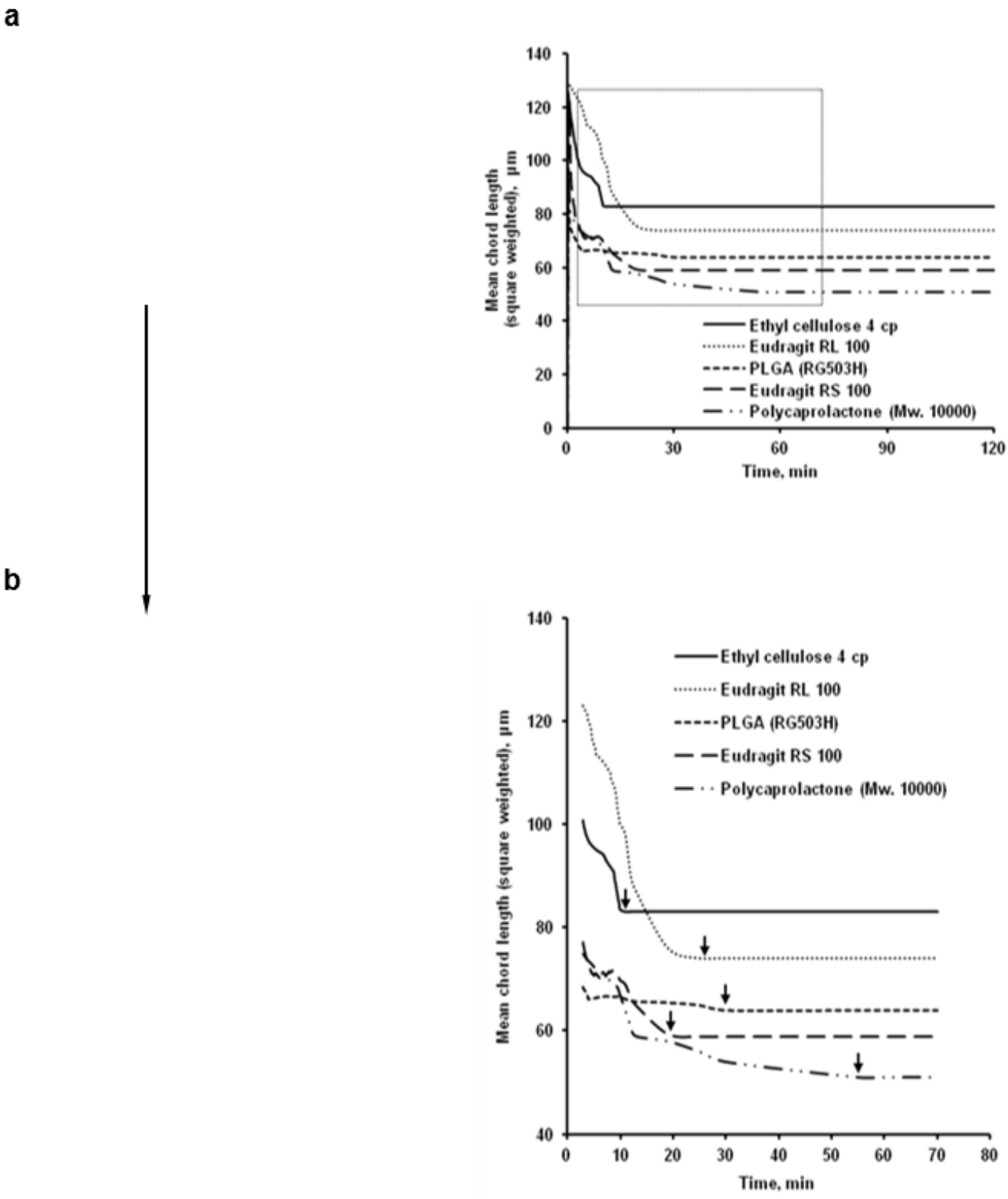

Figure 1

Effect of polymer type on square weighted mean chord length during microparticle formation by O/W method [(a) whole process and (b) hardening time of microparticle; arrow (↓): starting time of microparticle hardening]

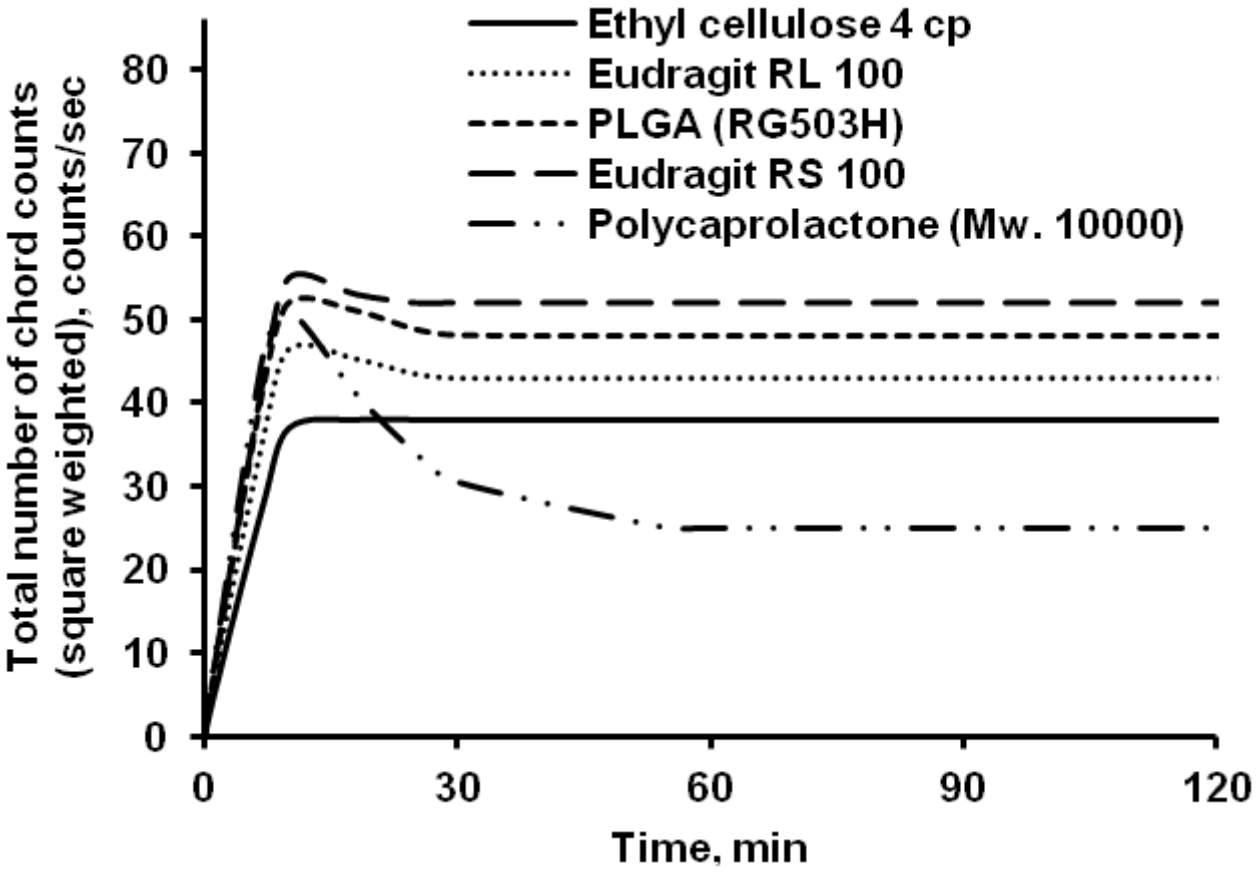

Figure 2

Effect of polymer type on the number of chord counts (square weighted) during solvent evaporation process

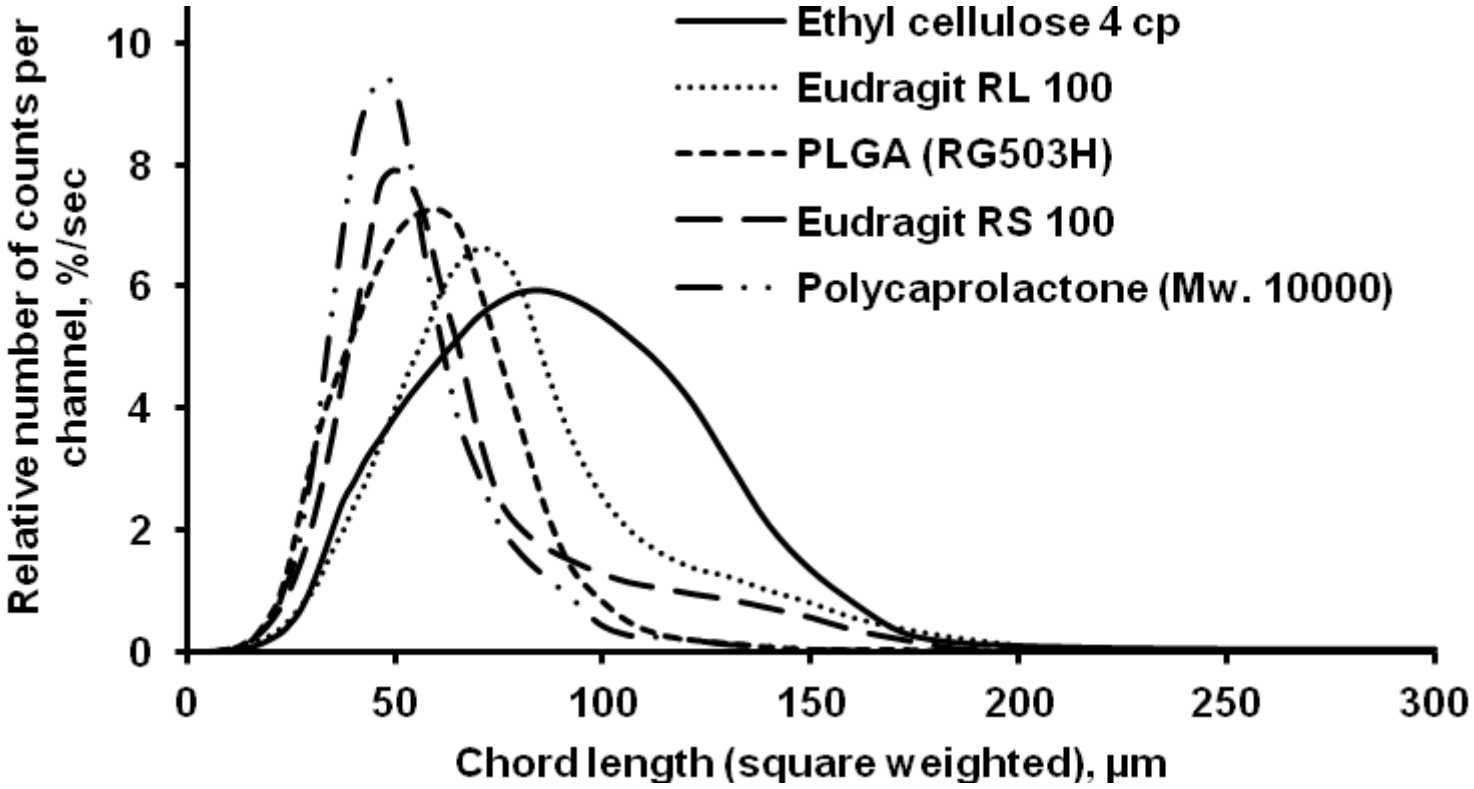

Figure 3

Effect of polymer type on the square weighted chord length distributions, (particle size distribution) at 4 hours stirring time

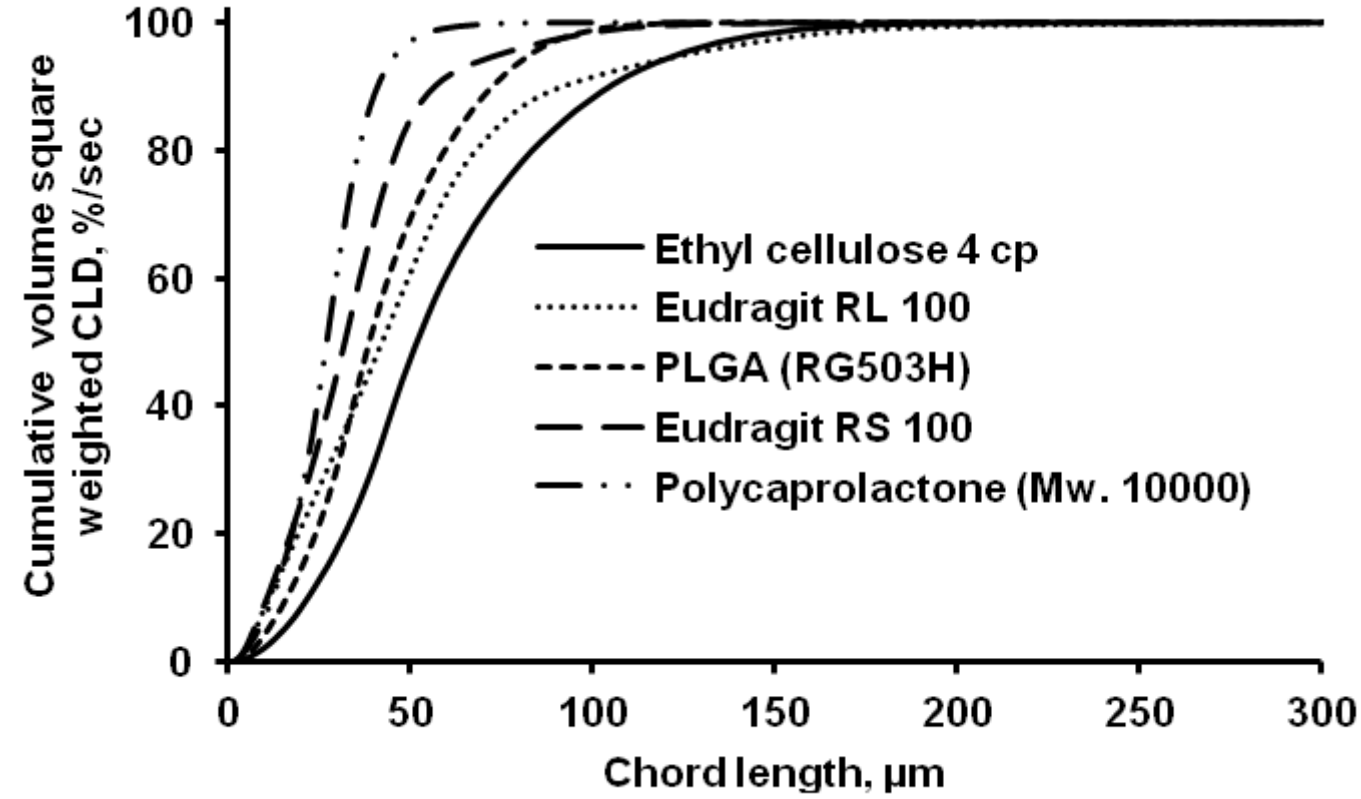

Figure 4

Comparison of the square weighted chord length distribution for various polymer obtained by the FBRM method (O/W) [at 4 hours stirring time]

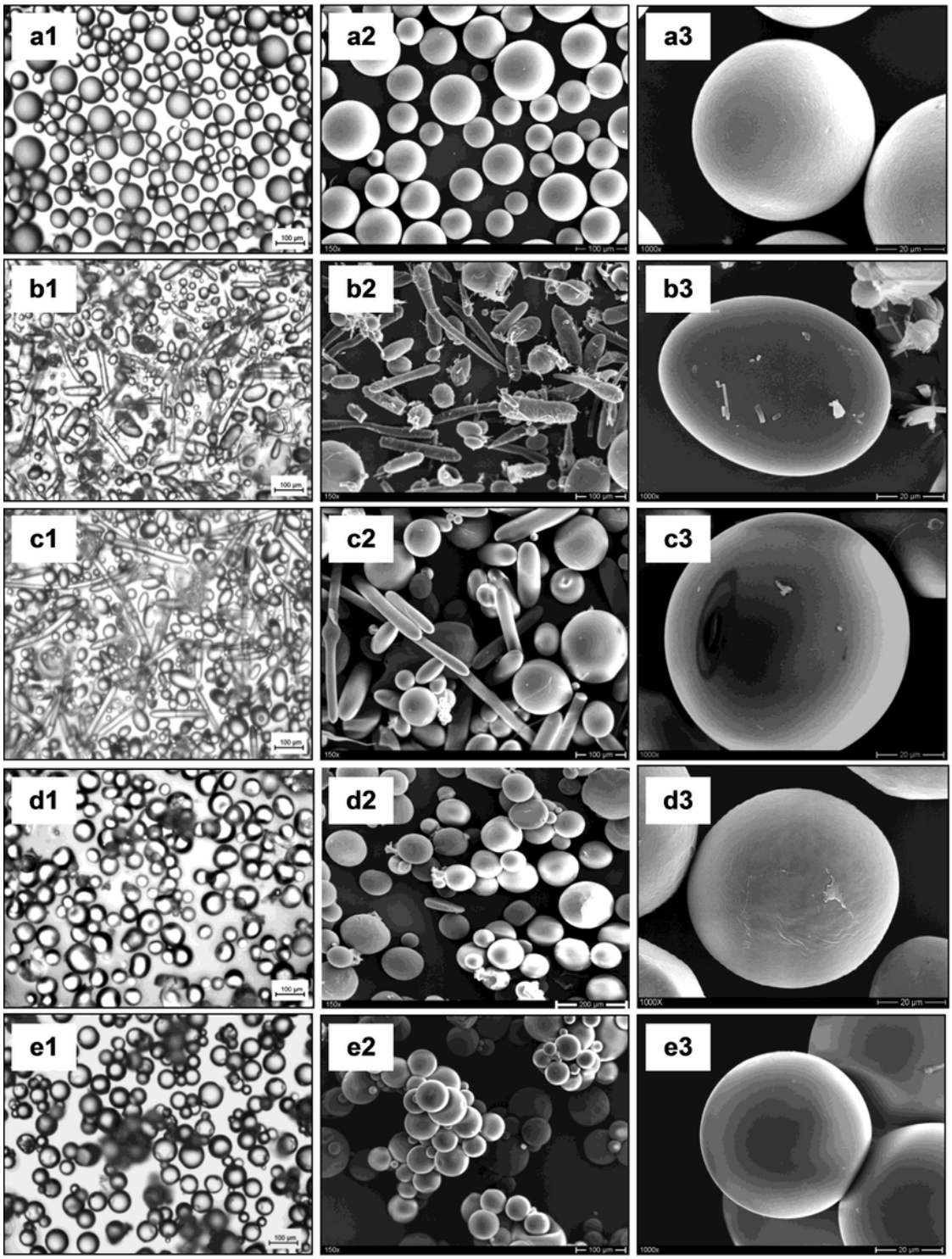

Figure 5

Optical microscopy pictures (1) and SEM pictures of polymeric microparticles (2. at 150x magnification & 3. at 1000x magnification) [a. Ethyl cellulose 4 cp; b. Eudragit RL 100; c. Eudragit RS 100; d. Polycaprolactone (Mw. 10000); e. PLGA (RG503H)].

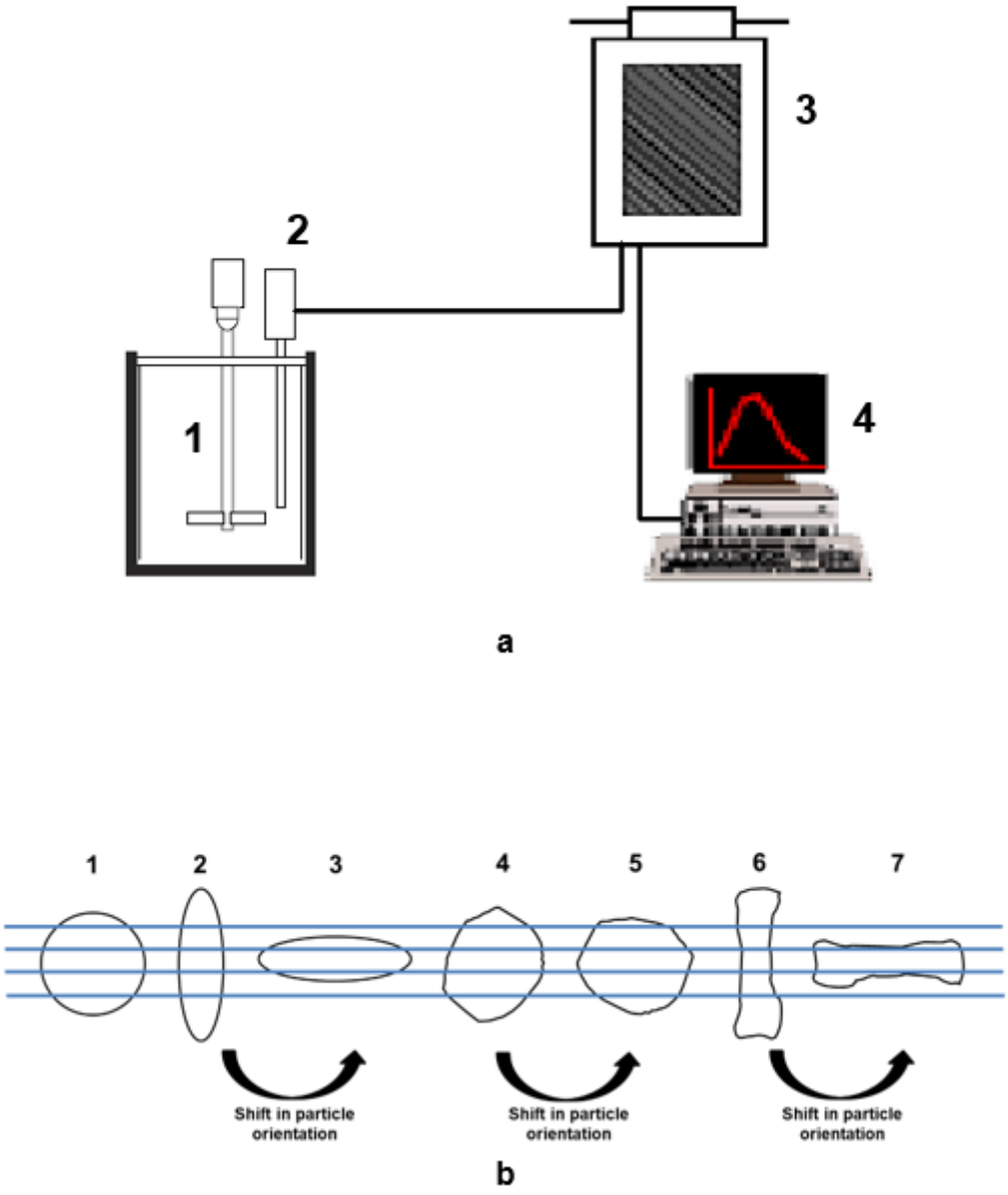

Figure 6

Schematic drawing of probe positioning relative to the impeller (1. Propeller stirrer; 2. Lasentec FBRM probe; 3. Processing unit; 4. PC monitoring the particle size distribution on-line) (a), and Examples of the measured chord length (line) when a laser beam crosses (1) a spherical particle, (2 and 3) an oval particle in different positions and (4, 5, 6 and 7) an irregular particle in different positions – illustration of the effect of particle orientation on the obtained chord length (b).